

Microstructure and Properties of Sn-Pb Solder Joints with Sn-Bi Finished Components

P. Snugovsky, J. McMahon, M. Romansky
Celestica Inc.

L. Snugovsky, D. Perovic, J. Rutter
University of Toronto
Toronto, Ontario, Canada

Abstract

For this study, researchers from the University of Toronto produced samples of Sn-Pb solder, with additions of bismuth, solidified at controlled cooling rates. The microstructure of the various Bi content and cooling rate combinations is analyzed. Limiting conditions for the occurrence of the Sn-Pb-Bi ternary eutectic are discussed. A team from Celestica produced two sets of test vehicle assemblies using both Pb-free and eutectic SnPb solder. The first set of assemblies includes combinations of three PWB surface finishes (OSP, Immersion Ag, ENIG) and three component lead finishes (Sn-Pb, Sn-Bi, Ni-Pd-Au). Microstructures, intermetallic type, composition, and thickness after assembly, aging, and 0°C to 100°C thermal cycling were studied. Pull testing was performed on QFPs and TQFPs to evaluate the tensile strength of solder joints as assembled and after thermal aging and vibration conditioning. The second set of assemblies was subjected to 6000 ATC cycles 0C to 100C. Results are provided for TQFP 0.5 mm and TQFP 0.4 mm devices on ENIG boards. The conclusions on combinations of solder pastes, surface finishes and component terminations are discussed.

Introduction

Because of the Pb-free implementation in the electronics industry and the European RoHS directive, many component manufacturers are changing finishes from Sn-Pb to alloys that do not contain Pb. Unfortunately, pure Sn coatings may grow tin whiskers, which could electrically short across component terminals. Alloying tin with a second metal reduces the propensity for whisker growth. Bismuth is considered to be an effective whisker suppressant. When used in Pb-free solder assembly processes, Sn-Bi is a viable candidate for component finishes. Sn-Bi coating is the most popular choice in Japan. However, some concerns exist in using Sn-Bi finishes in SMT processes that still employ eutectic Sn-Pb solder. They relate to low temperature equilibria that exist in the Sn-Pb-Bi system. The Bi content in the surface finish should be low enough in order to prevent formation of a low melting (96°C) ternary eutectic composed of the Sn, Bi and X phases (where X represents ternary phase that occurs in this alloy system) and also a ternary quasiperitectic with 137°C liquid formation. The questions always asked are:

“What is this equilibrium concentration?”

“What is the maximum Bi content in the alloy composition that will prevent any harmful segregation during freezing?”

In spite of excellent studies published [1] that addressed these concerns and the absence, as far as the authors are aware, of any papers reporting reliability problems with Sn-Bi finishes, the perception of danger in Bismuth surface finishes persists. Therefore, authors decided to run their own study. This study consists of three parts and is discussed in this paper. The first part is devoted to consideration derived from the ternary phase diagram and formation of microstructure under different cooling rates. The second and third parts relate to studies that were performed on test vehicles and concerned mechanical properties and fatigue life under thermal cycling 0°C to 100°C, respectively.

Experimental

The first part of the study reported here was intended to investigate this question from the microstructural point of view and, in addition, to provide information concerning alloys of higher Bi content as potential low melting solders.

Small samples of the alloys studied, contained in an aluminum crucible, were solidified by controlled withdrawal from a tube furnace. The cooling rate was obtained from the temperature – time curve of a thermocouple contained in the crucible assembly. Samples were mounted in epoxy for metallography, ground on successively finer silicon carbide papers, followed by polishing with 6 and 3 μm diamond abrasive and finished with colloidal silica.

The test vehicle for the second part of the study was designed to simulate mid-range board layouts (Figure.1). It incorporates double sided SMT placements, PTH manual placements, bottom-side SMT glue placement and chip-cap wave solder attachment.

The boards were 6 layers, built with high temperature FR4 epoxy laminate. Three different surface finishes were used including OSP, Immersion Ag (ImAg), Electroless Ni / Immersion Au (ENIG). The dimensions of the test vehicle were 210 mm x 335.3 mm x 1.6 mm. To simulate representative component mixes on mid-range complexity assemblies, 15 different component types were placed on the boards (Figure 2). No-clean solder pastes containing Sn-3.8%Ag-0.7%Cu were used for comparison with a standard eutectic Sn-Pb no-clean paste. The study was focused on the leaded components shown in Table 1.

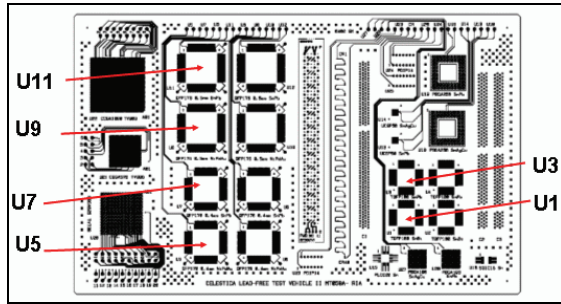


Figure 1 - Test Vehicle RIA1 Design

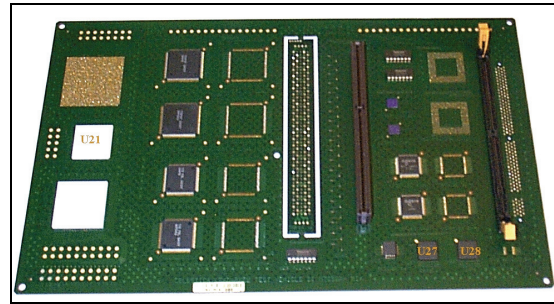


Figure 2 - Assembled Board RIA1

Table 1 - Component Description.

Component Type	I/O	Pitch, mm	Component Finish
TQFP, location U1	100	0.5	Sn-Bi
TQFP, location U3	100	0.5	Sn-Pb
QFP, location U5	176	0.4	NiPdAu
QFP, location U7	176	0.4	Sn-Pb
QFP, location U9	176	0.5	NiPdAu
QFP, location U11	176	0.5	Sn-Pb

Two reflow profiles were generated to accommodate eutectic Sn-Pb and Pb-free solder conditions. The reflow oven used for the assembly was a BTU Paragon 150 with 10 zones. The reflow was done using no clean pastes in an air atmosphere. As-assembled boards were aged at 125°C for 1000 hr

Leaded components (QFPs and TQFPs) were pull tested before and after vibration, and after aging. An Instron model 4502 was used. The crosshead speed was 2.5mm/min. Ten leads minimum were pulled for each component. Optical and SEM analyses of fracture surfaces were performed to determine the failure mode.

The influence of Sn-Bi finish on solder joint behaviour under thermal cycling was investigated on the RIA1 and RIA2 assemblies. The RIA2 test vehicle design for the third part of the study is shown in Figure 3.

Dimensions of the test vehicle were 203 mm x 253 mm x 2.36 mm. The boards had 12 layers of copper and were constructed with ENIG, ImAg, and OSP finishes on a high temperature Pb-free compatible laminate material. The discussion in this paper is limited to ENIG results.

To simulate representative component mixes on highly complex assemblies, 20 different component types were placed on the boards (Figure 4). This paper focuses primarily on the TQFP 0.5mm and TQFP 0.4mm packages.

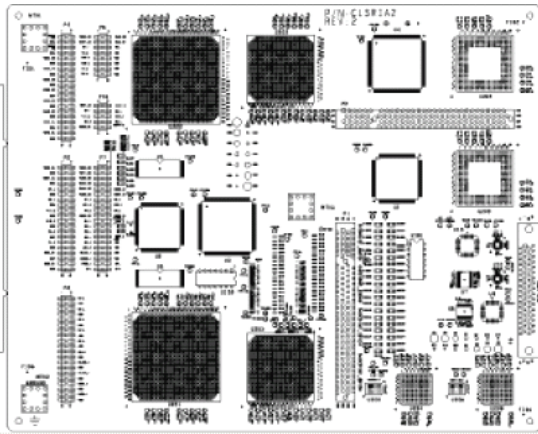


Figure 3 - Test Vehicle RIA2 Design

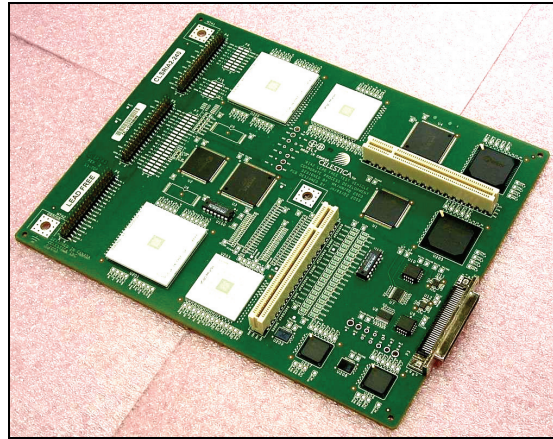


Figure 4 - Assembled Board RIA2

The assembly process included SMT and Wave. Two different reflow profiles were generated to accommodate Sn-Pb and two Pb-free solder conditions. Assembly was performed using no clean pastes in a nitrogen atmosphere using a BTU Paragon 150, 10 zone oven. All unpopulated cards were pre-conditioned through the same reflow profile to mimic a double-sided SMT process.

Thermal cycling 0°C to 100°C of the assembled test boards RIA1 and RIA2 was performed in a Blue M Environmental stress chamber. The ATC profile is shown in Figure 5. In RIA1, the boards of each set were removed from the chamber after 500, 1000, 1500, and 2000 cycles for analysis. In RIA2, 6010 cycles were completed before the testing was terminated. 17 boards were assembled for both Sn-Pb and Pb-free profiles so each of the legs had 16 cards (total of 32 components of each type).

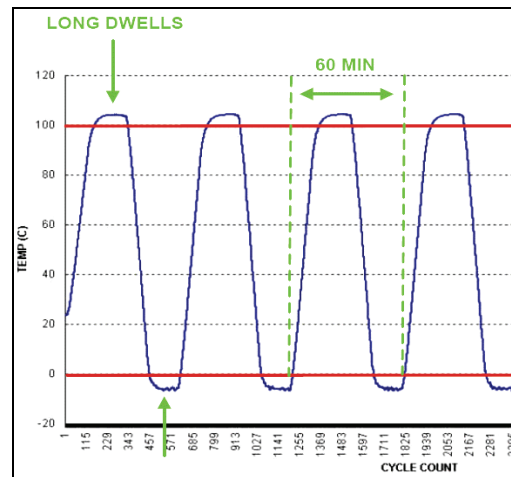


Figure 5 - Thermal Couple Reading of a Test Board

As-assembled and thermal cycled solder joints were examined before and after cross-sectioning using:

- Optical microscopy
- X-ray (Phoenix PCB analyzer)
- Scanning Electron microscopy (SEM, Hitachi S-4500 and SEM Hitachi S-3000N)
- X-ray spectroscopy (Oxford EDX)

Results and Discussion

The Bi-Pb-Sn Alloy System

The liquidus projection of the Bi-Pb-Sn system is shown in Figure 6 [2]. Two of the bounding binary systems, Pb-Sn and Bi-Sn, are simple eutectic systems, while the Bi-Pb system is more complex, having both eutectic and peritectic reactions. The ternary system shows several four-phase invariant equilibria, which lead to the corresponding reactions, including ternary eutectic (E) and ternary peritectic (P) reactions and two quasiperitectic reactions, U_1 and U_2 . Reaction U_1 takes the form $Pb+L = Sn+\square$ and U_2 corresponds to $\square L=Sn+X$. These reactions, including the corresponding phase compositions, are listed

in Table 2 [2]. Note also that one phase, denoted the X phase, formed during freezing of certain compositions, undergoes ternary eutectoid decomposition on cooling in the solid state. The tie quadrilaterals corresponding to the two quasiperitectic reactions, U_1 and U_2 , are shown on the liquidus projection of Figure 6. The tie quadrilateral for reaction U_1 is outlined by the points Pb-Sn- U_1 (L)- β Pb and that for U_2 by β Sn- U_2 (L)-X- β . Sample compositions that lie within these tie quadrilaterals will undergo some quasiperitectic reaction during freezing, so that freezing will not be complete until temperatures of 137°C, corresponding to reaction U_1 , or lower are reached.

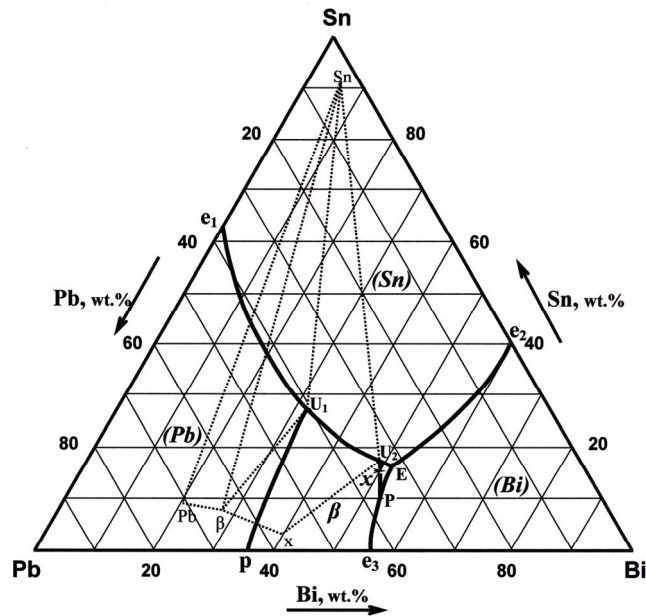


Figure 6 - Liquidus Projection of The Bi-Pb-Sn Alloy System. (After Osamura [2])

Table 2 - Ternary Reactions of The Bi-Pb-Sn Alloy System [2]

Reaction	Temperature, °C	Phase	Composition, wt.%		
			Bi	Pb	Sn
U_1	137.4	L	32.6	40.8	26.6
		(Pb)	20.0	70.6	9.6
		β	27.9	63.9	8.2
		(Sn)	5.4	2.9	91.7
	132	L	30	40	30
P	103	L	53	37.5	9.5
		X	41	56	3
U_2	99	L	50	32.5	17.5
E	96	L	52	32	16
		X	39.5	57.0	3.5
		(Bi)	99.0	0.5	0.5
		(Sn)	13.5	0.8	85.7

Effects of Bi Additions:

A number of effects of the addition of Bi to the Pb-Sn binary eutectic alloy can be derived from the ternary phase diagram. From Figure 6 is seen that the addition of Bi to the Pb-Sn eutectic alloy will change the alloy composition on a line directed from the binary eutectic point to the Bi corner of the ternary diagram. This line intersects the U_1 quadrilateral at approximately 11 weight percent Bi. Consequently, no quasiperitectic reaction U_1 is expected for Bi content less than that value. Note also that this composition variation does not follow the Pb-Sn monovariant eutectic valley: rather, the formation

of primary Sn phase is expected to result from the Bi addition, as well as the development of a freezing range. Also, the addition of Bi will influence the nucleation behaviour of the alloy. Normally, the Pb phase of the eutectic nucleates first on cooling, requiring only a small under cooling for its initiation, and it then acts as a good nucleation catalyst to initiate freezing of the Sn phase [2]. However, the introduction of Bi lowers the liquidus temperature for the Pb phase. This effect can be estimated by extrapolation, using the isotherms shown in the original equilibrium diagram of reference [2]. The result of this procedure is shown in Table 3.

Table 3 - Estimated Liquidus Temperatures for The Sn and Pb Phases Resulting from Bi Additions

Weight % Added Bi	Liquidus Temp For Pb phase, °C	Liquidus Temp For Sn phase, °C	Undercooling for Pb phase nucleation, °C
0	183	183	0
3	170	181	11
6	150	179	29

Consequently, enough undercooling may be developed to nucleate the Sn phase first, causing recalescence and forming primary Sn dendrites. Nucleation of the Pb phase is delayed, since Sn is not a good catalyst for nucleation of the Pb phase [3].

Experimental Observations:

For reference, the microstructure of a sample of Pb-Sn eutectic alloy, containing no added Bi, solidified at a cooling rate of 1.2°C per second is shown in Figure 7. It is seen to have the lamellar microstructure, with eutectic colonies, typical of this alloy.

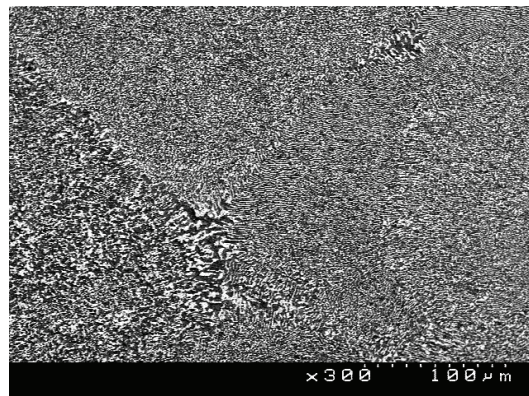


Figure 7 - Typical Lamellar Microstructure of Pb-Sn Eutectic Alloy Solidified at a Cooling Rate of 1.2°C per Second (SEM Backscatter Image)

The microstructure of a sample of Pb-Sn eutectic alloy with 3 weight percent of Bi added, solidified at various cooling rates, is shown in Figure 8. Only the Pb and Sn phases are present, having the lamellar microstructure. However, the eutectic colonies are substantially smaller than those in the Bi-free sample, decreasing in size with increasing cooling rate, and there is much more coarse material in the colony boundaries. The differential scanning calorimetry (DSC) heating curve of Figure 9 indicates a freezing solid-liquid range (i.e. equilibrium freezing range) of approximately 8°C for this alloy composition.

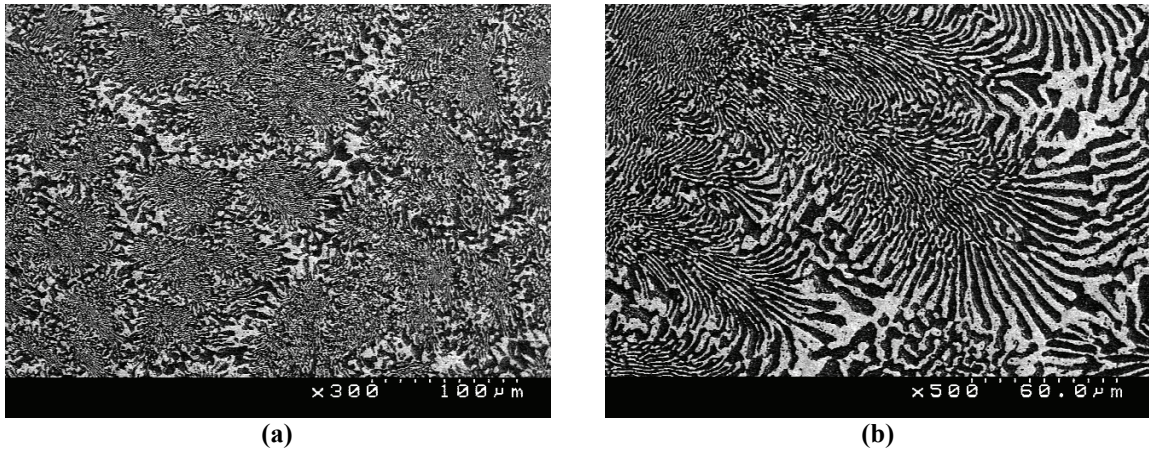


Figure 8 - Microstructures of Pb-Sn Eutectic Alloy with 3 Weight Percent Added Bi (SEM Backscatter Images)
(a) Cooling rate 5.5°C per second, (b) Cooling rate 0.5°C per second.

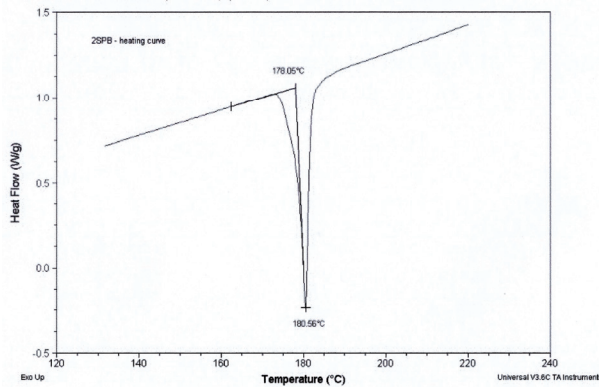


Figure 9 - DSC Heating Curve for Sample of Pb-Sn Eutectic Alloy with 3 Weight Percent Added Bi
Curve indicates freezing range of approximately 8°C for this alloy.

The microstructure of a sample containing 6 weight percent added Bi, solidified at various cooling rates, is shown in Figure 10. In this case, the microstructure was observed to be more strongly dependent on cooling rate, consisting of many primary Sn dendrites, with interdendritic eutectic regions at low cooling rates (Figure 10(a)) and progressively fewer Sn dendrites at higher cooling rates (Figures 10(b) and 10(c)). Again, only the Pb and Sn phases were observed, as expected from the phase diagram. The DSC heating curve for a sample of this composition is shown in Figure 11: a freezing range (i.e. equilibrium freezing range) of approximately 12°C is indicated by this curve.

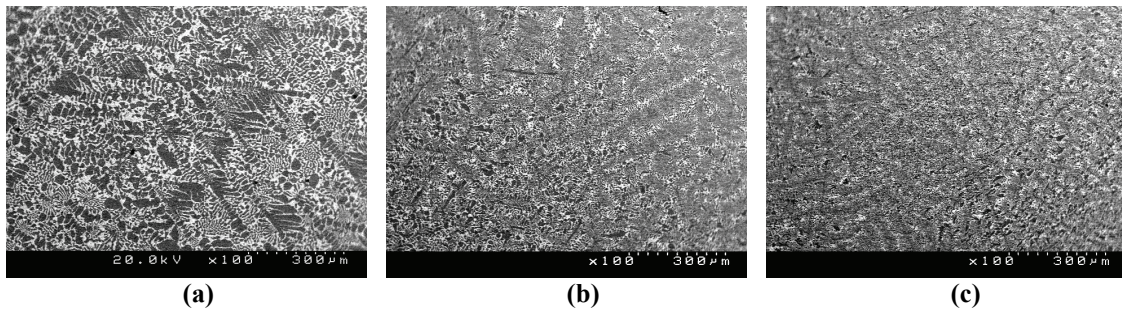


Figure 10 - Microstructure of Samples Pb-Sn Eutectic Alloy with 6 Weight Percent Added Bi
Backscatter SEM images
(a) Cooling rate 0.33°C per second (b) Cooling rate 3.3°C per second
(c) Cooling rate 4.8°C per second.

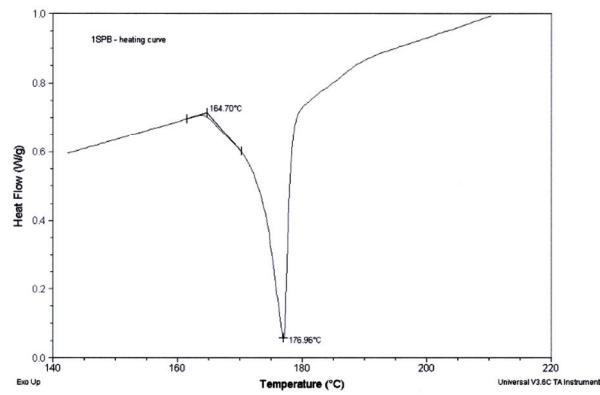


Figure 11 - DSC Heating Curve for Sample Pb-Sn Eutectic Alloy with 6 Wt.% Added Bi
 A freezing range (i.e. equilibrium freezing range) of approximately 12°C is indicated by this curve.

The microstructure of a sample containing 15 weight percent added Bi, solidified at a cooling rate of 2.8°C per second, is shown in Figure 12. The predominant feature of this microstructure is seen to be the presence of many Sn dendrites, which appear somewhat fragmented in Figure 12. In addition to the Pb and Sn phases, the \square phase was found in the microstructure, formed as a result of the quasiperitectic reaction U_1 . The presence of that phase is indicated by a substantial response in the DSC heating curve of Figure 13 at the U_1 quasiperitectic temperature of 137°C. This curve indicates a freezing range of approximately 27°C for this alloy composition. No reactions at temperatures lower than 137°C were detected for this alloy composition.

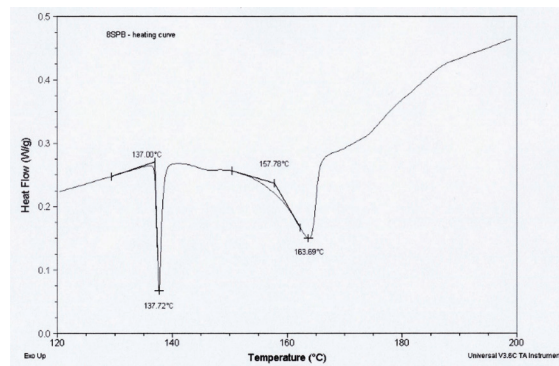
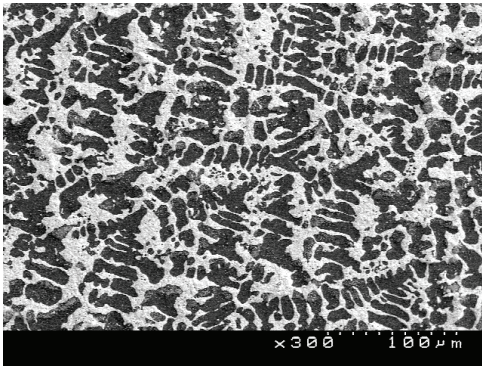


Figure 12 - Microstructure of a Sample of Pb-Sn Eutectic Alloy with 15 Wt% added Bi, Cooled at 2.8°C per Second (SEM Backscatter Image) **Figure 13 - DSC Heating Curve for Sample of Pb-Sn eutectic alloy with 15 wt.% added Bi. Note thermal response at 137°C, indicating quasiperitectic reaction U_1 . A freezing range of approximately 27°C was measured.**

Lower Melting Compositions are not relevant to this paper and will be discussed late in a separate paper.

Mechanical & Metallurgical Properties

Representative sections through leaded components are shown in Figure 14. Wetting with Pb-free solder as well as with Sn-Pb solder meets the IPC-A-610-D specification target. Electroless Ni / Immersion Au finish is the best in terms of wetting. Immersion Ag performs better than OSP finish (ENIG > ImAg > OSP).

The minimum heel fillet height of all the components meets the IPC-A-610-D specification requirements. A difference in fillet formation is found in solder joints with different component terminations:

- On Sn-Pb and Sn-Bi lead finishes both Sn-Pb and Pb-free solders wick up
- On NiPdAu, both Sn-Pb and Pb-free solders do not wick up, have higher contact angle than with the Sn-Pb finish, and have higher heel fillet height.

Both X-ray and cross-section followed by SEM analysis were employed to characterize voiding. It was found that all QFPs have voiding measured below 12% and they are small.

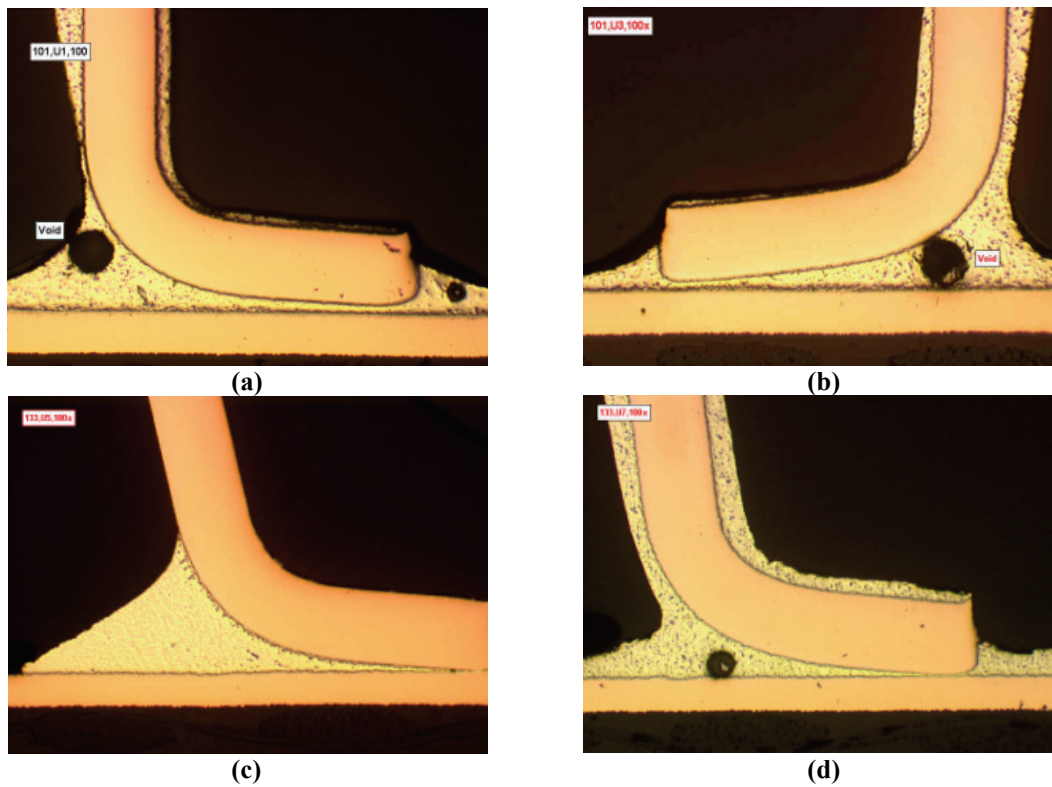


Figure 14 - Pb-Free Solder Joint Fillets with Different Board and Lead Finishes at 100 X: (a) ENIG – Sn-Pb Finish; (b) ENIG – Sn-Bi Finish; (c) OSP – NiPdAu Finish; (d) OSP – Sn-Pb Finish

The solder joints formed with conventional Sn-Pb solder on Pb-free finishes and Pb-free component terminations may have microstructures different from the eutectic Sn-Pb microstructure (Figure 15). On all analyzed board finishes: OSP, ImAg, and ENIG with NiPdAu component termination, Pb-primary crystals form in solder. Sn-primary crystals are clearly visible in Sn-Pb solder joints with Sn-Bi component finish on all board finishes.

Sn-Pb solder joints with Sn-Bi lead finished components were carefully examined using SEM and EDX. The purpose of the analysis was to insure that the low melting structure containing Bi-Pb compound particles was not formed during crystallization. The Bi content in component finish is 3%. The estimated dilution for completely dissolved plated layer is 10 times. The resulting solder joint composition is 66%Sn, 34%Pb and 0.3%Bi. The typical microstructure for analyzed solder joints made with Sn-Bi finished components is shown in Figure 15(b). It consists of Sn-primary dendrites and Sn-Pb eutectic. Bi is dissolved in Sn during crystallization.

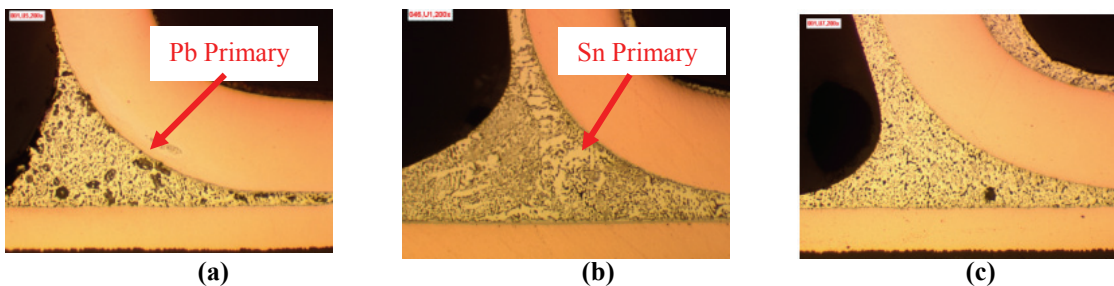


Figure 15 - Sn-Pb Solder Microstructure with Different Component Finishes, 200 X: (a) NiPdAu Finish; (b) Sn-Bi Finish; (c) Sn-Pb Finish

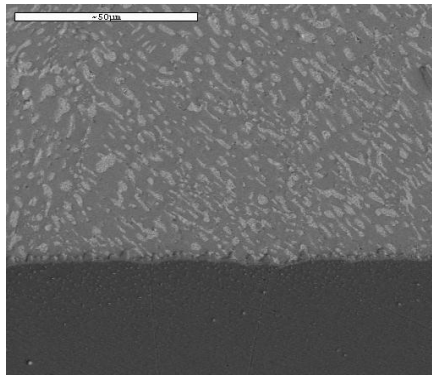


Figure 16 - Sn-Pb Solder Microstructure with Sn-Bi Finish, SEM, 1000 X

The Pb-free solder joints with NiPdAu, and Sn-Bi, finishes have a typical near eutectic composition microstructure. It consists of Ag_3Sn plates, Sn dendrites, and Sn-Ag-Cu eutectic (Figure 17a).

Pb-free solder joint microstructure with Sn-Pb component finish contains Pb that forms Sn-Ag-Pb ternary eutectic (Figure 17b), in addition to the three phases above. This eutectic melts at $177^\circ C$. Therefore these solder joints have a pasty range of more than $10^\circ C$.

In solder joints with NiPdAu, Pd- and Au-containing intermetallic is found (Figure18).

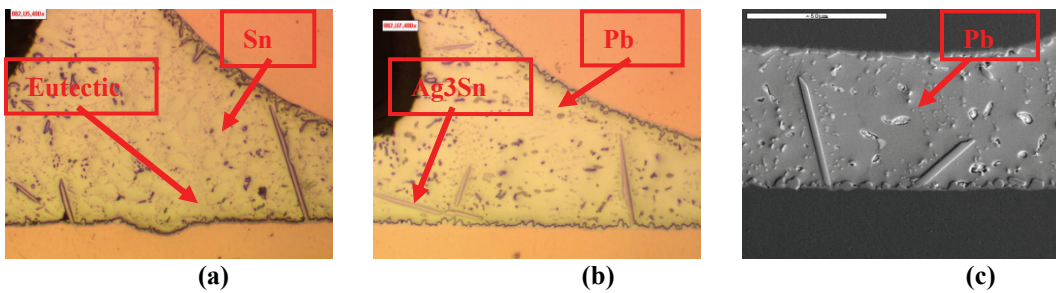


Figure17 - Pb-Free Solder Microstructure with Different Component Finishers:

(a) NiPdAu Finish, 400 X; (b) Sn-Pb Finish, 400 X; (c) Sn-Pb Finish, SEM, 1000 X

The solder joint microstructure may also contain intermetallic particles caused by pad material dissolution:

- Cu_6Sn_5 on OSP finished boards with all type of terminations
- $Cu_6Sn_5 + Ag_3Sn$ on Immersion Ag with all type of terminations
- Cu_6Sn_5 on ENIG finished boards with all Sn-Bi, or Sn-Pb finished components
- No additional intermetallic particles on ENIG with NiPdAu

In Sn-Pb solder, the Ni_3Sn_4 type of intermetallic is formed as a reaction layer between the ENIG finished pad and Sn-Pb solder. Interfacial Ni_3Sn_4 intermetallic grows in arrays of platelets. In lead-free solder, the intermetallic type formed between the ENIG finished pads and solder is Me_6Sn_5 , where $Me = Cu$ and Ni . If the solder joint forms between Cu (OSP and Immersion Ag finished boards) and solder (both Sn-Pb and Pb-free), the Cu_6Sn_5 type of intermetallic grows. This intermetallic usually has a scalloped surface.

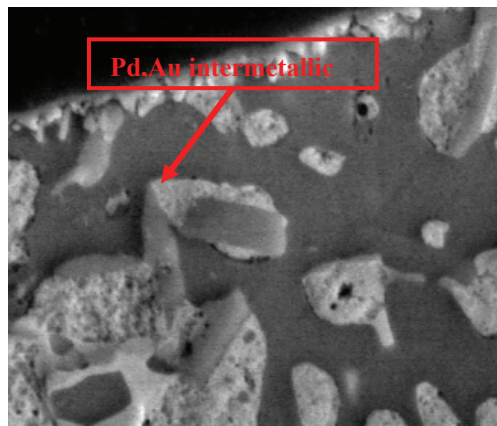


Figure 18 - Sn-Pb Solder Joint with NiPdAu Component Finish, SEM, 5,000 X

The “As built” intermetallic layer is slightly thicker in Pb-free solder joints than in Sn-Pb, both board-side and component-side. The intermetallic thickness in solder joints formed on ENIG boards is lower than in joints on Immersion Ag and OSP finished boards. The component - side intermetallic is thinner on NiPdAu than on Sn-Pb finish.

During aging, the intermetallic thickness increases. The intermetallic layer is always thicker after aging, both board-side and component-side, and for both Pb-Sn and Pb-free solder. Intermetallic thickness for Pb-free solder is typically greater than that of Pb-Sn solder. The board-side intermetallic thickness is typically greater than the component-side intermetallic thickness. As a result of aging, the intermetallic / solder interface is flattened in both Pb-free and Sn-Pb solder joints. Cu_3Sn intermetallic grows during aging in both Pb-free and Sn-Pb solder joints formed on OSP and Immersion finished boards

The aging process promotes grain growth and coalescence of the particles by diffusion, which results in coarsening of the microstructures in both the Pb-free and Pb based solder joints. The Pb-free solder joint microstructure coarsens more slowly than Sn-Pb.

The microstructure after aging depends on the surface finish:

- ENIG – $(Cu, Ni)_6Sn_5$ continue to grow consuming Cu atoms from solder. Almost no Cu is left in solder joints after aging. Bulk solder composition transforms from Sn-Ag-Cu to Sn-Ag resulting in a microstructure without Cu-based intermetallic particles.
- OSP and Immersion Ag – the Cu continues to dissolve in the solder, resulting in a thickening intermetallic layer and also in increasing Cu content in bulk solder. The microstructure contains many Cu_6Sn_5 particles.

Lead pull testing results from the following conditions were compared:

- Sn-Pb eutectic solder vs. Pb-free solder from the same vendor.
- Three PWB surface finishes: OSP, Immersion Ag, and ENIG
- Three component finishes, Sn-Pb, Sn-Bi, and NiPdAu

The various combinations of these conditions represent pure Sn-Pb systems, pure Pb-free systems and mixed conditions expected during the transition to pure Pb-free processes.

Analysis of Variance tools were used to compare the pull strength in Newtons (N) on samples of the 18 combinations at three conditions. Pull tests were performed on samples in the as built condition, after temperature aging and after vibration conditioning. There are a total of 741 individual samples and 53 treatments. Each treatment includes a minimum of 10 pull tests.

Two failure modes were identified (Figure 19). The predominant failure mode is cohesive failure through the bulk solder. The second failure mode identified is adhesive failure, where the pad was pulled from the board indicating that the strength of the solder joint exceeded the bond strength between pad and board. This failure mode, identified as “Pad Lift” did not occur on these devices in the as built condition, but represents a small portion of the results for aged and vibration lots. This failure mode has a censoring effect on the data, by limiting the maximum failing strength of individual solder connections.

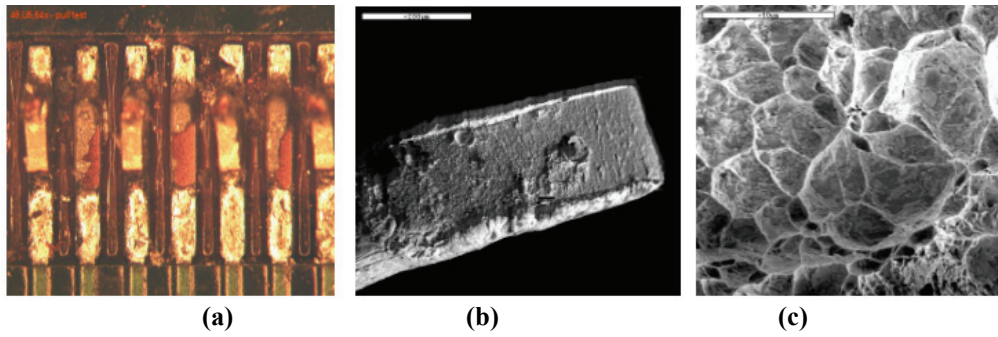


Figure 19 - Fracture Surface after Adhesive Failure and Through Solder:

(a) Adhesive Failure – Lift-Pad; (b) Failure Through Solder, SEM, 130 X; (c) Failure Through Solder, SEM, 1,000 X

The grand average for all samples is 7.49 N and there are statistically significant differences in lot means across all of the analyzed factors as well as interesting interactions between condition and plating systems. The pull test results are shown in Figures 20.

Pb-free solder joints have higher strength than eutectic Sn-Pb in all of the tested conditions, despite having overall thicker intermetallic layers. This was an expected result based on the respective microstructures. The small Ag_3Sn and Cu_6Sn_5 particles in the Pb-free solder increase the strength of the solder joint and impede the growth of the Sn grains. In addition, lattice strains are established at the precipitation matrix interface, creating a distortion of the crystal lattice in the vicinity of these particles. During plastic deformation, dislocation motion is impeded as a result of these distortions. Consequently, the solder becomes harder and stronger to some degree. The pull strength is lower after aging due to grain growth and intermetallic layer growth. The pull strength is higher after vibration due to strain hardening under low stress deformation.

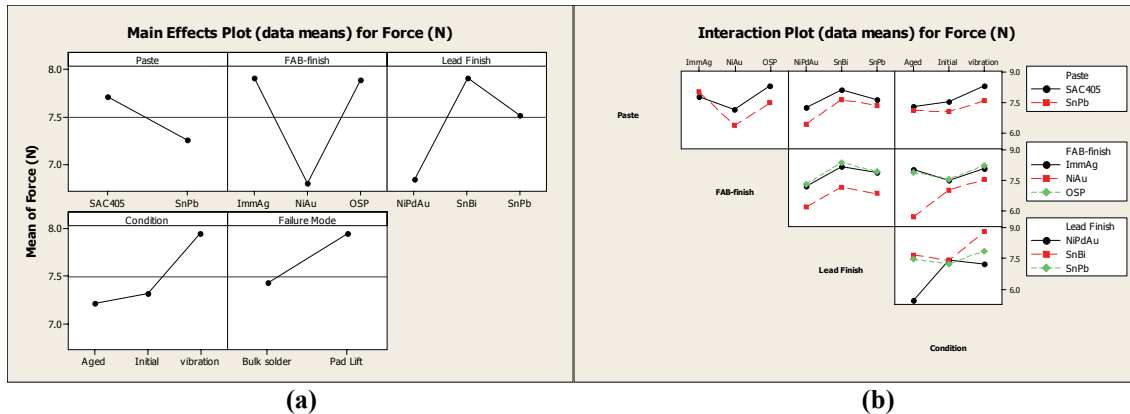


Figure 20 - Lead Pull Test Force (N), as-Assembled, Aged, and After Vibration Solder Joints
(a) Main Effect Plot (b) Interaction Plot

The PWB surface finish has a significant effect on pull strength. The ENIG finish has lower strength in all conditions but also appears to be more susceptible to aging. There are multiple reasons for the lower strength. Sn-Pb solder forms Ni_3Sn_4 which is more brittle than the Cu_6Sn_5 formed by OSP and ImAg. Cu_6Sn_5 formed in the SAC alloy consumes Cu and the resulting solder joint composition increases grain growth. There is also the possibility of a Black Pad effect. The Ni corrosion was detected on some ENIG finished boards.

The Sn-Bi lead finish generated higher average pull strengths than both Sn-Pb and Ni-Pd-Au using both SAC405 and Sn-Pb paste, for all board finishes, at all of the tested conditions.

Thermal Cycling Reliability

In leaded components, coarsened bands are formed near the leads in Sn-Pb solder joints on all the finishes and components terminations. No significant coarsening was detected in all analyzed Pb-free solder joints.

In Sn-Pb solder joints, the most stable microstructure forms with the Sn-Bi component finish on all three (OSP ImAg, and ENIG) board finishes (Figure 21). Grains are larger with the Sn-Pb finish than with Sn-Bi, and even larger with Ni/Pd/Au. The coarsest microstructure is typical for the Ni/Pd/Au finish.

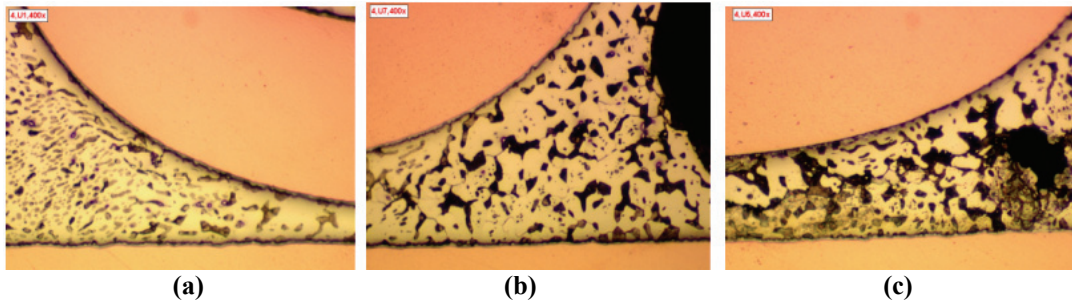


**Figure 21 - TQFP Sn-Pb Solder Joint Microstructure after 2000 Cycles at 0 – 100°C:
(a) Sn-Bi Finish; (b) Sn-Pb Finish; (c) NiPdAu Finish**

Damage of leaded components starts similarly in both Sn-Pb and Pb-free solder joints: heel areas are deformed as shown in Figure 22. Then small cracks appear. The cracks in Pb-free solder joints are narrower than in Sn-Pb joints. The cracks propagate through the solder close to the leads. In terms of cracking in Pb-free solder, the worst combination is Pb-free solder with Sn-Pb component finish on all analyzed surface finishes. This is attributed to the Pb segregation in the narrow space between the pad and the lead [4]. Failures were detected in these joints after 2000 cycles at 0 – 100°C. In Sn-Pb solder no fully cracked joints were found with Sn-Bi finished components after 2000 cycles.

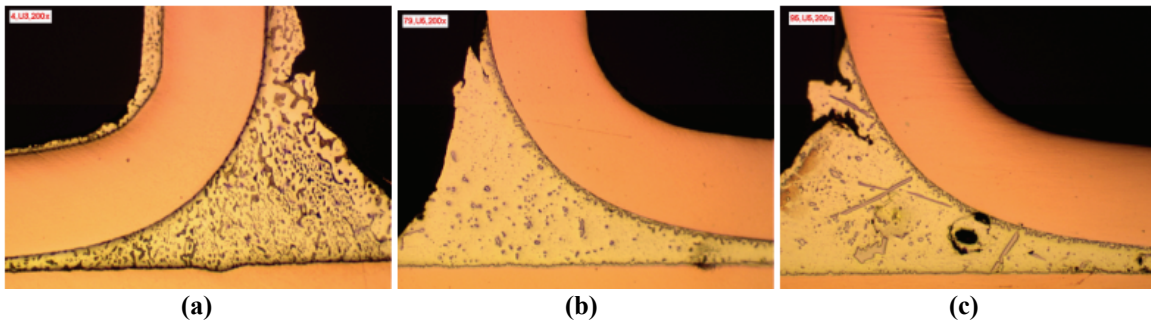


**Figure 22 - TQFP Microstructure after 2000 Cycles at 0 – 100°C:
(a) Sn-Pb Solder, OSP, Sn-Pb Finish; (b) Pb-Free Solder, OSP, Sn-Pb Finish;
(c) Pb-Free Solder, ImAg, Ni/Pd/Au Finish**

In the RIA2 study, no open joints were found with Sn-Bi finished TQFPs after 6010 cycles in either Sn-Pb and Pb-free solder. The typical microstructures are shown in Figure 23.

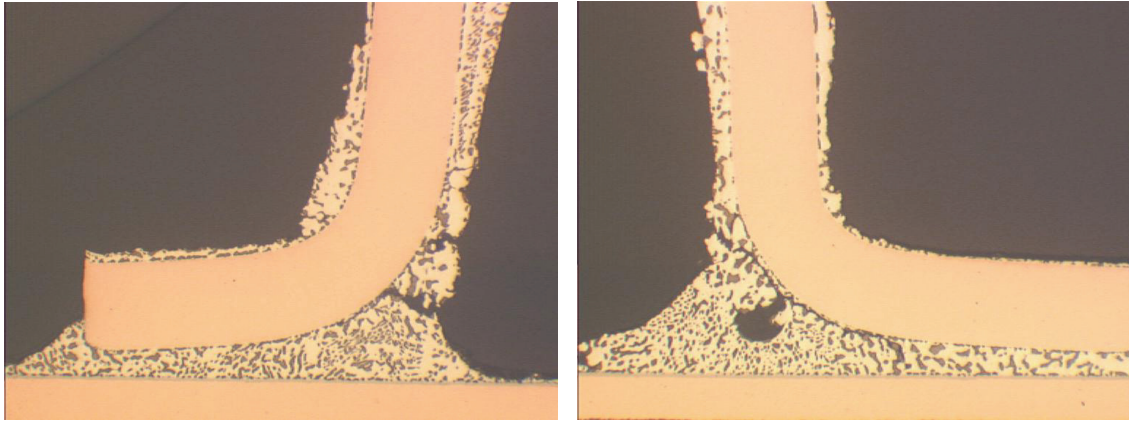


Figure 23 - Sn-Pb Solder Joint Microstructure with Sn-Bi Finished Components after 6010 Cycles at 0 – 100°C, ENIG Finish: (a) TQFP 0.5mm; (b) TQFP 0.4mm.

Conclusions

- The low melting reactions does not occur in the near eutectic Sn-Pb alloys with Bi additions up to 6% at the cooling rates employed at SMT processes. Therefore, there is no danger in using Sn-Bi finished components with Bi content up to 6%, that create final solder joints with Bi content 5 -10 times lower.
- Sn-Bi lead surface finish provides the highest pull strength in both Pb-free and Sn-Pb solder joints. It also stabilizes Sn-Pb joint microstructure during thermal cycling, reducing the grain growth and preventing crack formation.
- Pb-free solder joints are stronger than Sn-Pb joints in all of the tested conditions: as assembled, after vibration, and after aging.
- Ni/Pd/Au, Sn-Bi, and Sn-Pb component lead finishes exhibited very similar strengths in as-assembled conditions. But after aging, Pb-free and Sn-Pb solder joints with Ni/Pd/Au component finish have significantly lower pull strength than others.
- TQFP 0.5mm and 0.4mm with Sn-Bi finish form reliable Sn-Pb solder joints with an excellent fatigue life.
- Sn-Pb lead plating using with Pb-free solder reduces the fatigue life and should be avoided even in the transition period or for the exempted products.

Acknowledgements

The authors would like to thank the following individuals from Celestica: Zohreh Bagheri for cross-sectioning and microstructure analysis, George Riccitelli for the pull test experiment and Russell Brush for ATC testing and data analysis.

References

1. J. S. Hwang, “Bismuth in Lead-free Systems – Not to Fear”, SMT, June 2005, p.14. www.smtmag.com.
2. P. Villars, A. Prince, and H. Okamoto, editors, “Handbook of Ternary Alloys Phase Diagrams”, Vol. 5 (Materials Park, OH:ASM Int., 1995), pp. 6373-6780.
3. K. W. Moon, W. J. Boettinger, U. R. Kattner, C. A. Handwerker, and D.J. Lee, “The Effect of Pb Contamination on the Solidification Behavior of Sn-Bi Solder”, Journal of Electronic Materials, Vol. 30, No. 1, 2001, pp. 45 – 52.
4. K. Seelig, D. Suraski, “Lead-Contamination in Lead-Free Electronics Assembly”, www.aimsolder.com